PAPER

Coordination chemistry of sterically encumbered pyrrolyl ligands to chromium(II): mono(pyrrolyl)-chromium and diazachromocene formation†

Markus Kreye, Constantin G. Daniliuc, Matthias Freytag, Peter G. Jones and Marc D. Walter*

A series of diazachromocenes with sterically demanding pyrrolyl ligands, $2,5\text{-}(Me_3C)_2C_4H_2N$ (**1**), $2,5\text{-}(Me_3C)_2\text{-}3,4\text{-}Me_2C_4N$ (**2**) and $2,3,5\text{-}(Me_3C)_3C_4HN$ (**3**), was prepared and investigated by various spectroscopic techniques, and in some cases by X-ray diffraction and magnetic susceptibility studies. The diazachromocenes exhibit an $S = 1$ ground state; no indication of a spin-equilibrium was obtained. With the same ligands mono(pyrrolyl)chromium(II) complexes are accessible, $[\{(\kappa N\text{-}2,5\text{-}(Me_3C)_2C_4H_2N)Cr\text{-}(thf)\}_2(\mu\text{-}Cl)_2]$ (**1-CrCl(thf)**), $[\kappa N\text{-}2,5\text{-}(Me_3C)_2\text{-}3,4\text{-}Me_2\text{-}C_4H_2N)Cr(Cl)(tmeda)]$ (**2-CrCl(tmeda)**) and $[(\eta^5\text{-}2,3,5\text{-}(Me_3C)_3C_4HN)Cr(\mu\text{-}Cl)_2]$ (**3-CrCl**), which show either η^5- or $\eta^1\text{-}(\kappa N)$ coordination depending on the substitution pattern. ^1H NMR spectroscopy serves as a valuable tool to distinguish between these coordination modes. The Cr(II) atoms in the mono(pyrrolyl) complexes adopt a high spin configuration ($S = 2$) and in dimeric species antiferromagnetic coupling between the spin carriers was observed. However, none of these mono(pyrrolyl)chromium complexes is an effective or selective ethylene oligomerization catalyst on activation with MAO or $AlMe_3$, supporting the importance of a Cr(I)/Cr(III)-based catalytic cycle.

Introduction

Transition metal complexes bearing heterocyclopentadienyl ligands have been of interest for some time.[1–7] An interesting feature associated with these ligands is their ability to participate in $\eta^5 \rightarrow \eta^3 \rightarrow \eta^1$ ring slippage processes. In homogeneous catalysis this isomerization might represent an advantageous feature. In the case of pyrrolyl, the N atom facilitates this switch,[8] and pyrrolyl complexes with η^5- and $\eta^1\text{-}(\kappa N)$ coordination are well documented in the literature.[6,7,9,10] However, in many cases the coordination mode is dictated by the Lewis-acidity of the metal atom.

Surprisingly, while studies on pyrrolyl chromium(II) and chromium(III) complexes date back to 1966,[11,12] structurally well-characterized species were first reported by Gambarotta in 1990 using pyrrolyl and 2,5-dimethylpyrrolyl as ligands, for which $\eta^1\text{-}(\kappa N)$-coordination was observed exclusively.[13] Interestingly, chromium pyrrolide catalyst systems generated from $Cr[O_2CCH(Et)(Bu)]_3$, 2,5-dimethylpyrrole and $AlEt_2Cl/AlEt_3$

Institut für Anorganische und Analytische Chemie, Technische Universität Braunschweig, Hagenring 30, 38106 Braunschweig, Germany.
E-mail: mwalter@tu-bs.de; Fax: +49 531-391-5309

exhibit high activity and excellent selectivity in ethylene trimerization to 1-hexene.[14,15] The origin of this selectivity, and also the question as to which intermediates are involved in this process, have been the focus of extensive studies.[14,15] One important aspect was to establish which chromium species is responsible for the high selectivity of the trimerization, since under the employed reaction conditions catalytic cycles involving Cr(I)/Cr(III) or Cr(II)/Cr(IV) intermediates are feasible. DFT calculations have been undertaken, but could support either possibility.[16] However, more recent *in situ* EPR monitoring of the trimerization process supports the formation of Cr(I) and Cr(II) species, whereby only Cr(I) is catalytically relevant.[17] Furthermore, Gambarotta and Duchateau used the more sterically encumbered 2,5-di-*tert*-butylpyrrolyl for this reaction and prepared the Cr(III) complex $[(\eta^5\text{-}2,5\text{-}(Me_3C)_2C_4H_2N)CrCl_2(thf)]$. On addition of $AlEt_3$ at low temperature the dinuclear Cr(III) species $[\{(\eta^5\text{-}2,5\text{-}(Me_3C)_2C_4H_2N)CrEt\}_2(\mu\text{-}Cl)_2]$ was formed, which acts as a single-component, self-activating precatalyst for ethylene trimerization. The authors also isolated the catalytically inactive dinuclear Cr(II) complex $[\{(\kappa N\text{-}2,5\text{-}(Me_3C)_2C_4H_2N)Cr(thf)\}_2(\mu\text{-}Cl)_2]$ from the reaction of $[\{(\eta^5\text{-}2,5\text{-}(Me_3C)_2C_4H_2N)CrEt\}_2(\mu\text{-}Cl)_2]$ with $AlEt_3$.[18] Both observations further strengthen the hypothesis of a Cr(I)/Cr(III) catalytic cycle.
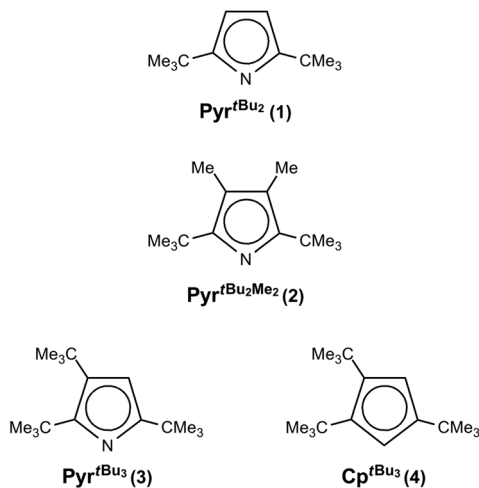
Nevertheless, from a structural point of view the κN-coordination for the latter compound is surprising, since *tert*-butyl

Me₃C, CMe₃

Pyr^tBu₂ (1)

Me, Me
Me₃C, CMe₃

Pyr^tBu₂Me₂ (2)

Me₃C, CMe₃
Me₃C, CMe₃

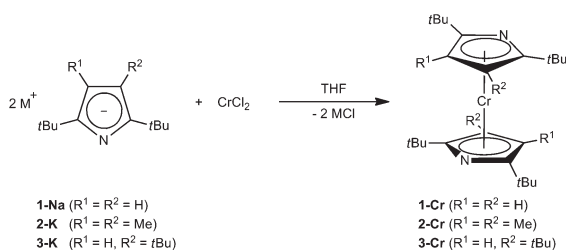**Pyr^tBu₃ (3)**

Me₃C, CMe₃
Me₃C, CMe₃

Cp^tBu₃ (4)

Chart 1

(tBu) groups in 2,5-positions of the pyrrolyl framework generally sterically disfavour η¹-coordination but instead η⁵-coordination is observed.[6,7,19,20] Recently, we have initiated a research program on sterically encumbered pyrrolyl systems with an emphasis on comparing them with their cyclopentadienyl analogues, with respect to their ability to stabilize half-sandwich complexes.[21–23] Herein, we report our observations on the coordination chemistry of bulky pyrrolyls (Chart 1) with Cr(II) and briefly discuss the reactivity of pyrrolyl chromium(II) half-sandwich complexes in the polymerization/oligomerization of ethylene.

Results and discussion

Synthesis and characterization of diazachromocenes

For Cr(II), η⁵-coordination of pyrrolyl ligands is rarely observed and requires the functionalization of the N-lone pair, e.g., by methylation[24] or coordination by Lewis-acids such as AlMe₃.[25] However, based on our previous investigations on azatrozircenes[22] and diazaferrocenes[23] we anticipated that the sterically encumbered pyrrolyl ligands **1–3** would behave similarly to their cyclopentadienyl analogues. Indeed, the reaction of pyrrolides **1-Na**, **2-K** and **3-K** with CrCl₂ in a 2:1 ratio in THF yields the corresponding red bis(pyrrolyl)chromium(II) complexes **1-Cr**, **2-Cr** and **3-Cr**, respectively (Scheme 1).

2 M⁺ [pyrrolide] + CrCl₂ →(THF, − 2 MCl) [bis-pyrrolyl Cr complex]

1-Na (R¹ = R² = H)   **1-Cr** (R¹ = R² = H)
2-K (R¹ = R² = Me)   **2-Cr** (R¹ = R² = Me)
3-K (R¹ = H, R² = tBu) **3-Cr** (R¹ = H, R² = tBu)

Scheme 1

These complexes are very soluble in aliphatic hydrocarbons, in which they form red solutions, and crystals of **1-Cr** and **2-Cr** suitable for X-ray diffraction were grown from concentrated pentane or hexane solutions at −24 °C (Table 1).

However, because of its high solubility, crystals of **3-Cr** had to be grown from a saturated hexamethyldisiloxane solution at −24 °C. The ¹H NMR spectra of these complexes feature broad resonances between δ 5 and −1 ppm at ambient temperature. Nevertheless, for **1-Cr** and **3-Cr** only the tBu resonances were observed, while the methine CH protons are too broad to be detected (see the Experimental section for details). For comparison, in the ¹H NMR spectrum of [(η⁵-1,3-(Me₃C)₂C₅H₃)₂Cr] the tBu-groups resonate at δ 0.2 (ν₁/₂ = 250 Hz) and no methine resonances were found.[26] Furthermore, the UV/vis spectra of **1-Cr**, **2-Cr** and **3-Cr** resemble each other closely, consistent with the notion that the pyrrolyl ligands **1–3** exhibit similar ligand field strengths (see ESI† for details).

The molecular structures of **1-Cr** (which displays crystallographic twofold symmetry) and **2-Cr** (which displays approximately twofold symmetry, r.m.s.d. 0.20 Å) are shown in Fig. 1 and 3, and selected bond distances and angles are listed in the figure caption. The electron delocalization within a pyrrolyl system can be readily deduced from the individual CC bond distances, which are intermediate between the distances of isolated single (d^0(C–C) = 1.54 Å)[27] and double (d^0(C=C) = 1.34 Å)[27] bonds. To quantify the extent of delocalization within the heterocyclic ring, the parameter $τ$[28–30] was defined as the normalized quotient of the single and double bond lengths (eqn (1)).

$$\tau = 1 + \frac{\left(\dfrac{d(\text{C}-\text{C})}{d(\text{C}=\text{C})}\right) - 1}{1 - \left(\dfrac{d^0(\text{C}-\text{C})}{d^0(\text{C}=\text{C})}\right)} \qquad (1)$$

A completely delocalized system such as benzene adopts a $τ$ value of 1, while $τ$ approaches 0 for a localized system.[28–30] For **1-Cr** and **2-Cr** $τ$ values are 0.97 and 1.00, respectively, suggesting complete electron delocalization. Furthermore, as expected from the NMR spectroscopy, the molecular structure of **1-Cr** is closely related to that of the cyclopentadienyl derivative [(η⁵-1,3-(Me₃C)₂C₅H₃)₂Cr],[26] which shows a Cp(cent)–Cr distance of 1.81 Å. This bond distance is also similar to that (1.80 Å) of [(η⁵-1,2,4-(Me₂CH)₃C₅H₂)₂Cr]. Structurally it is also related to the hexaphosphachromocene, [(η⁵-2,3-(Me₃C)₂C₂P₃)₂Cr].[31] All these system complexes have an $S = 1$ ground state. For comparison, Cr(II) high spin ($S = 2$) complexes have significantly longer Cp(cent)–Cr distances, as shown for the mixed-sandwich complex [(η⁵-C₅Me₅)Cr(Tp)] (Tp = hydrotris(pyrazolyl)borate) (2.01 Å).[32,33]

However, because of intramolecular ligand repulsion, bulky Cp ligands can also favour longer metal–carbon bonds associated with the high spin state, e.g., [(η⁵-1,2,3,4-(Me₂CH)₄C₅H)₂Cr] is a low spin ($S = 1$) molecule in solution at ambient temperature,[34] but in the solid state a gradual spin-crossover from the $S = 1$ to the $S = 2$ state is observed.[35] To exclude this possibility for **1-Cr**, the solid state magnetic

Table 1 Crystallographic data

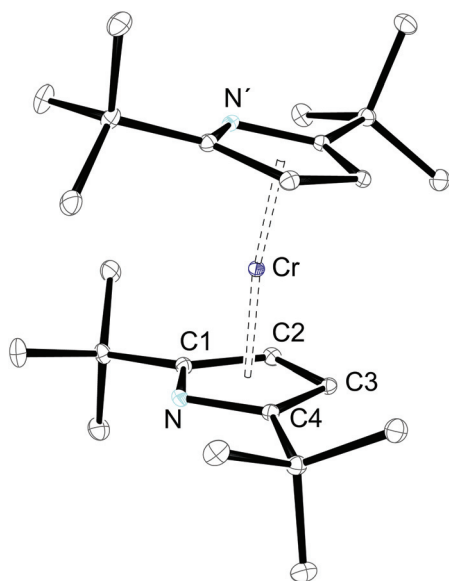| Compound reference	1-Cr	2-Cr	1-CrCl(thf)	2-CrCl(tmeda)	4-CrCl
Chemical formula	$C_{24}H_{40}CrN_2$	$C_{28}H_{48}CrN_2$	$C_{32}H_{56}Cl_2Cr_2N_2O_2$	$C_{20}H_{40}ClCrN_3$	$C_{34}H_{58}Cl_2Cr_2$
Formula mass	408.58	464.68	675.69	410.00	641.70
Crystal system	Tetragonal	Monoclinic	Monoclinic	Monoclinic	Triclinic
a/Å	8.6668(2)	9.0267(5)	8.0202(2)	9.6784(4)	10.2638(4)
b/Å	8.6668(2)	32.0929(16)	15.7066(4)	17.7933(7)	12.3091(6)
c/Å	30.8408(12)	10.4615(6)	14.2953(4)	12.8412(5)	13.8743(6)
α/°	90.00	90.00	90.00	90.00	89.431(4)
β/°	90.00	114.962(7)	103.847(4)	93.221(4)	88.919(4)
γ/°	90.00	90.00	90.00	90.00	89.248(4)
Unit cell volume/Å^3	2316.56(12)	2747.5(3)	1748.45(8)	2207.81(15)	1752.31(13)
Temperature/K	100(2)	130(2)	100(2)	100(2)	100(2)
Space group	$P(-4)2_1c$	$P2_1/c$	$P2_1/n$	$P2_1/n$	$P(-1)$
No. of formula units per unit cell, Z	4	4	2	4	2
Radiation type	Mo Kα	Cu Kα	Mo Kα	Cu Kα	Mo Kα
Absorption coefficient, μ/mm^{-1}	0.504	3.522	0.803	5.414	0.792
No. of reflections measured	87 304	59 471	68 193	46 931	49 059
No. of independent reflections	2764	5706	4169	4578	7693
R_{int}	0.0438	0.0990	0.0477	0.0618	0.0554
Final R_1 values ($I > 2\sigma(I)$)	0.0265	0.0587	0.0287	0.0745	0.0302
Final w$R(F^2)$ values ($I > 2\sigma(I)$)	0.0658	0.1482	0.0617	0.0732	0.0601
Final R_1 values (all data)	0.0279	0.0651	0.0358	0.0355	0.0569
Final w$R(F^2)$ values (all data)	0.0663	0.1538	0.0644	0.0770	0.0625
Goodness of fit on F^2	1.131	1.044	1.046	1.042	0.838
$\Delta\rho$/e Å^{-3}	0.266/−0.337	1.210/−0.707	0.340/−0.277	0.346/−0.313	0.334/−0.296

Fig. 1 ORTEP diagram of **1-Cr** with thermal displacement parameters drawn at 50% probability. The hydrogen atoms have been omitted for clarity. Selected bond lengths (Å): N–C1 1.3769(18), C1–C2 1.4254(19), C2–C3 1.4288(19), C3–C4 1.4208(19), C4–N 1.3874(17), Cr–N 2.1902(12), Cr–C1 2.1945(13), Cr–C2 2.1552(15), Cr–C3 2.1240(14), Cr–C4 2.1411(14), Pyr(cent)–Cr 1.80, Pyr(cent)–Cr–Pyr(cent) 172.3; τ 0.97; N–Pyr(cent)···Pyr′(cent)–N′ −85.3°.

Fig. 2 χ_T vs. T plot for **1-Cr**.

susceptibility was recorded between 2 and 360 K and the χ_T vs. T plot is shown in Fig. 2. The magnetic moment of $\mu_{eff} = 3.0\mu_B$ ($\chi_T \approx 1.12$ emu K) is temperature independent and consistent with an $S = 1$ ground state, and no evidence of spin-crossover behaviour can be gathered.

The introduction of the more sterically encumbered pyrrolyl **2** has only minor effects on the overall molecular structure and
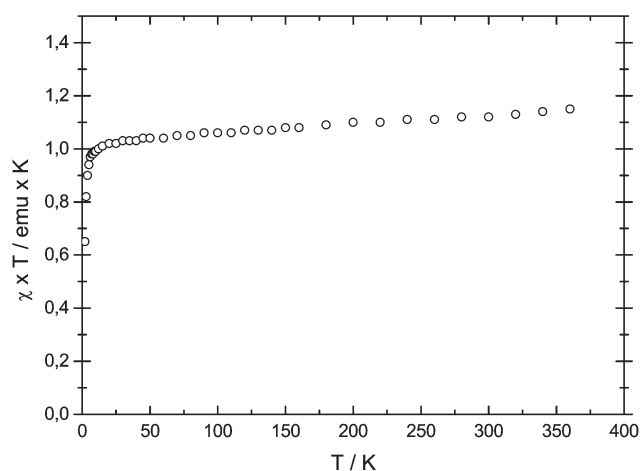
the Pyr(cent)–Cr distance (1.82 Å) is only slightly elongated (Fig. 3). Nevertheless, a closer inspection also reveals that the N-atom is better shielded in **2-Cr** than in **1-Cr**, since the additional methyl substituents in the 3,4-positions push the adjacent *tert*-butyl groups towards the nitrogen atoms, as shown by the average C(*t*Bu)–C–N angles of 119.3° and 120.6° for **2-Cr** and **1-Cr**, respectively.

X-ray investigations also established the qualitative molecular structure for **3-Cr**, but this could not be refined satisfactorily because no unambiguous differentiation between the N- and CH-positions within the pyrrolyl ring was possible.

Synthesis and characterization of mono(pyrrolyl)chromium complexes

The next question to be addressed is the influence of the pyrrolyl substitution pattern on the coordination modes in mono-
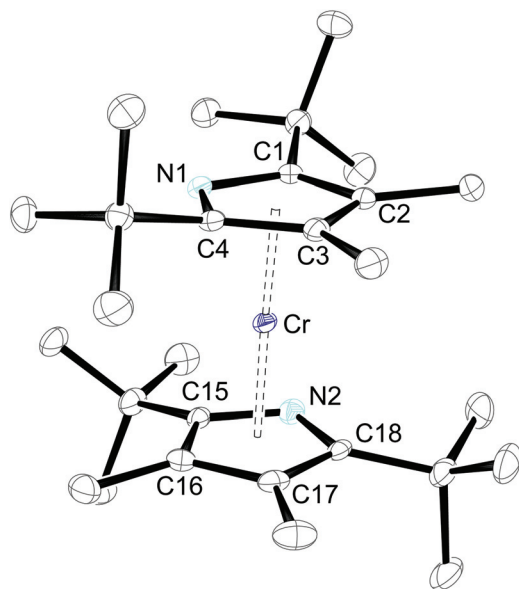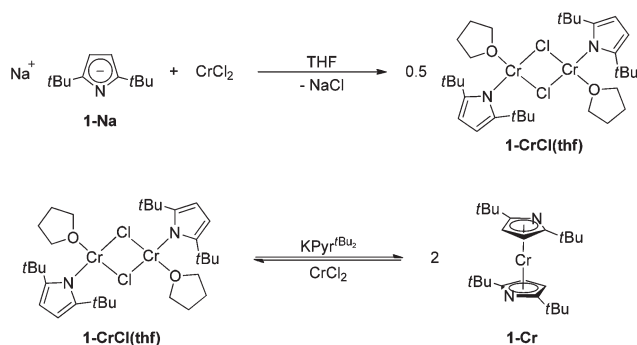
Fig. 3 ORTEP diagram of **2-Cr** with thermal displacement parameters drawn at 50% probability. The hydrogen atoms have been omitted for clarity. Selected bond lengths (Å): N–C1 1.395(3), C1–C2 1.421(3), C2–C3 1.422(4), C3–C4 1.426(3), C4–N 1.397(3), N2–C15 1.385(3), C15–C16 1.431(4), C16–C17 1.426(4), C17–C18 1.417(4), C18–N2 1.396(3), Cr–N1 2.095(2), Cr–C1 2.165(2), Cr–C2 2.259(2), Cr–C3 2.232(2), Cr–C4 2.132(2), Cr–N2 2.092(2), Cr–C15 2.148(2), Cr–C16 2.258(2), Cr–C17 2.259(2), Cr–C18 2.149(2), Pyr(cent)–Cr 1.82, Pyr(cent)–Cr–Pyr(cent) 174.3; τ 1.00; N1–Pyr1(cent)···Pyr2(cent)–N2 99.9°.
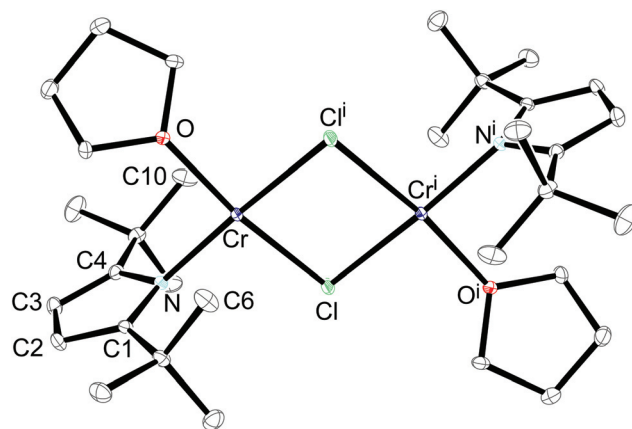

Scheme 2

Fig. 4 ORTEP diagram of **1-CrCl(thf)** with thermal displacement parameters drawn at 50% probability. The hydrogen atoms have been omitted for clarity. Selected bond lengths (Å) and angles (°): Cr–N 2.0176(11), Cr–O 2.0733(10), Cr–Cl 2.3902(4), Cr–Cl^i 2.3961(4), N–C1 1.3909(17), C1–C2 1.3813(19), C2–C3 1.411(2), C3–C4 1.381(2), C4–N 1.3864(17), Cr···Cr^i 3.49, Cr···C6 2.91, Cr···C10 2.97, O–Cr–Cl 171.93(3), N–Cr–Cl^i 172.76(4), N–Cr–Cl 93.76(3), Cl–Cr–Cl^i 86.257(14), O–Cr–Cl^i 88.55(3), N–Cr–O 92.17(4); τ 0.87.

(pyrrolyl)chromium(II) complexes. The reaction of **1-Na** with 1 equiv. of $CrCl_2$ in THF results in a blue solution, from which the previously reported complex [{(κN-2,5-(Me$_3$C)$_2$C$_4$H$_2$N)Cr-(thf)}$_2$(μ-Cl)$_2$] (**1-CrCl(thf)**)[18] can be isolated in good yield. The complex **1-CrCl(thf)** is only sparingly soluble in aliphatic and aromatic hydrocarbons, but has a good solubility in THF. Alternatively, **1-CrCl(thf)** can be prepared from the reaction of **1-Cr** with 1 equiv. of $CrCl_2$ (Scheme 2).

The different coordination modes in **1-CrCl(thf)** and **1-Cr** are immediately obvious when the ^{1}H NMR spectra of both compounds are compared. Whereas the tBu-groups in **1-Cr** are observed at δ 1.99 ($\nu_{1/2}$ = 121 Hz), they experience a dramatic downfield shift to δ 55.4 ($\nu_{1/2}$ = 2580 Hz). This behaviour can

be readily understood when one assumes that the paramagnetic chemical shift is dominated by the pseudo-contact term; that is, resonances closest to the paramagnetic centre display the greatest paramagnetic shifts and are also broader than those further away from the paramagnetic centre.[36] This also rationalizes the fact that the methine resonances are now observable at δ −28.4 ($\nu_{1/2}$ = 399 Hz). Overall, ^{1}H NMR spectroscopy offers a powerful tool for distinguishing κN- and η^5-coordination in these molecules. When **1-CrCl(thf)** is exposed to a dynamic vacuum for a prolonged period of time, the colour changes from blue to green and a poorly soluble material was obtained, precluding NMR spectroscopic analysis; but on addition of THF the blue colour is re-established. Unfortunately, at present we can only speculate on the identity of the green material, but the colour change might be related to a switch in the pyrrolyl coordination mode (from κN- to η^5-coordination).

Crystals of **1-CrCl(thf)** suitable for X-ray diffraction were grown by vapour diffusion of pentane into a concentrated THF solution at ambient temperature. The complex **1-CrCl(thf)** crystallized in the monoclinic space group $P2_1/n$ (Table 1), which is different from the previously reported rhombohedric space group R-3.[18] The conformation and orientation of the thf ligands are different in both polymorphs, whereas the bond distance and angles vary only slightly (see below).

An ORTEP diagram is shown in Fig. 4 and selected bond distances and angles are listed in the figure caption. The environment around the Cr^{2+} atom is square planar (sum of the angles: 360.7(1)°) and the two halves of the dimer are related by an inversion centre located in the middle of the Cr$_2$Cl$_2$-core. For steric reasons the pyrrolyl ligands are twisted out of the Cr$_2$Cl$_2$ plane by 87.7°. The Cr atom lies 0.8 Å outside the plane defined by the pyrrolyl moiety; in the rhombohedric
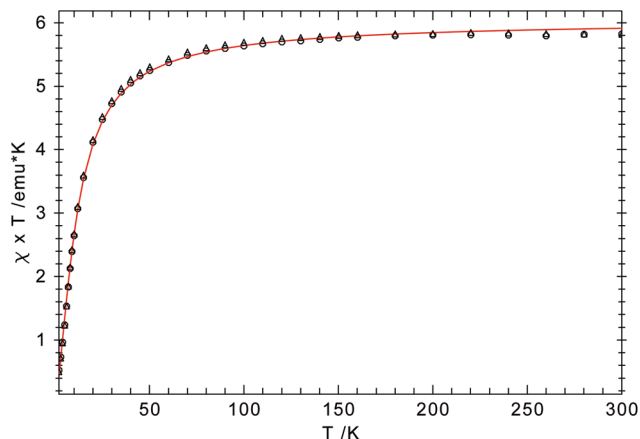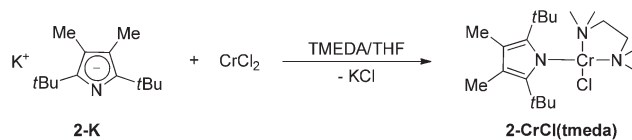
Fig. 5 χ_T vs. T plot for **1-CrCl(thf)**. Simulation: $S_1 = S_2 = 2$; $g_1 = g_2 = 2.01$; $J = 1.17$ cm^{-1}.
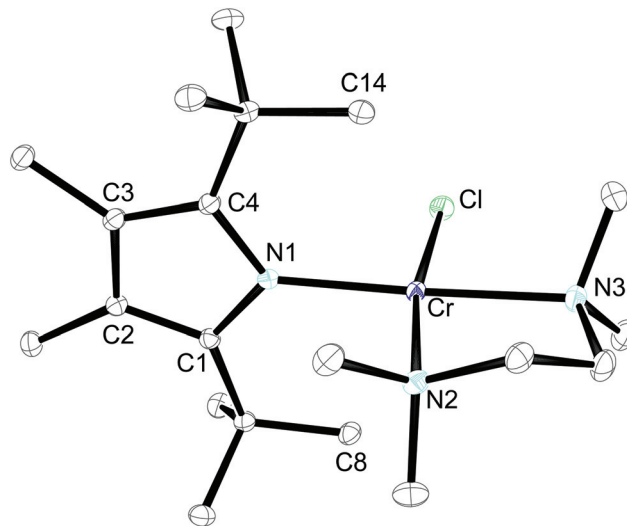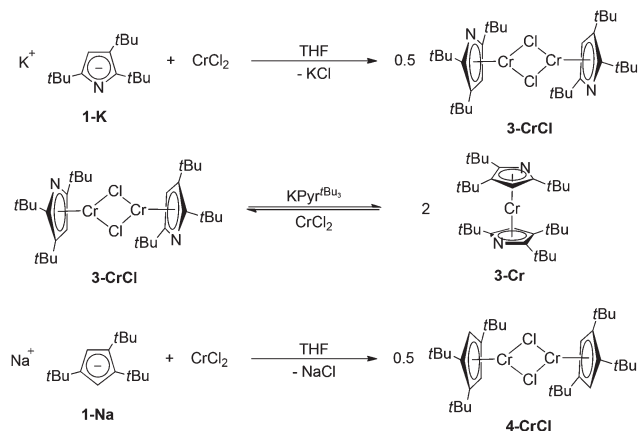

Scheme 3

Fig. 6 ORTEP diagram of **2-CrCl(tmeda)** with thermal displacement parameters drawn at 50% probability. The hydrogen atoms have been omitted for clarity. Selected bond lengths (Å) and angles (°): Cr–N1 2.0557(13), Cr–N2 2.2142(13), Cr–N3 2.1892(13), Cr–Cl 2.3646(4), N1–C1 1.3880(19), C1–C2 1.395(2), C2–C3 1.422(2), C3–C4 1.391(2), C4–N1 1.3921(19), Cr⋯C8 2.87, Cr⋯C6 2.81, N1–Cr–N2 95.86(5), N3–Cr–Cl 89.68(4), N1–Cr–N3 174.54(5), N2–Cr–N3 81.20(5), N1–Cr–Cl 93.31(4), N2–Cr–Cl 170.83(4), τ 0.86.

polymorph this displacement is only 0.39 Å.[18] Two relatively short non-bonding Cr⋯C distances (2.91 and 2.97 Å for Cr–C6 and Cr–C10, respectively) between one methyl group of the pyrrolyl tBu-groups are observed, providing additional steric protection of the fifth and the sixth coordination site of the Cr atom. The Cr–N distance of 2.0176(11) Å compares well with those of other reported Cr(II) amides.[13,37,38] A slightly shorter Cr–N distance (2.0121(19) Å) was found for the other polymorph.[18] In contrast to **1-Cr** and **2-Cr** the τ value of 0.87 for **1-CrCl(thf)** suggests a more localized electronic structure, as one would expect from κN-coordination, and it can be compared to that of the unsubstituted pyrrole ($\tau = 0.830$).[39] The long Cr⋯Cr^i distance of 3.49 Å precludes any Cr–Cr bond, and therefore electron exchange between the Cr(II) centres has to occur via the bridging Cl-atoms. Solid state magnetic susceptibility studies revealed that the Cr(II) atoms with a d^4 electron configuration adopt a high spin ($S = 2$) configuration and only a weak antiferromagnetic coupling is observed at low temperature. Fig. 5 shows the experimental data and the fit to the effective spin Hamilitonian $\hat{H} = -2J(\hat{S}_1 \cdot \hat{S}_2)$ (Fig. 5).

As pointed out above, the addition of two methyl groups at the 3,4-positions of the pyrrolyl systems increases the steric demand around the N-atom and therefore reduces its ability to coordinate in a κN-fashion. When **2-K** is treated with 1 equiv. of CrCl$_2$ in THF a steel-blue solution is formed, suggesting the formation of a mono(pyrrolyl) species analogous to **1-CrCl-(thf)**. However, when the solvent is removed, an additional colour change to red-brown is observed and only the diazachromocene **2-Cr** can be isolated on pentane extraction. However, on tmeda addition to the reaction mixture the monomeric Cr(II) complex **2-CrCl(tmeda)** can be crystallized from a concentrated THF solution at −24 °C (Scheme 3).

The ^{1}H NMR spectrum of **2-CrCl(tmeda)** exhibits similar features to that of **1-CrCl(thf)**, confirming the κN-coordination. This assumption was further substantiated by X-ray diffraction. The molecular structure of **2-CrCl(tmeda)** is depicted in Fig. 6 and selected bond distances and angles are listed in the figure caption. The Cr-atom is coordinated by one Cl-atom, the

bidentate tmeda ligand and pyrrolyl **2** in a square planar geometry. Two short non-bonding Cr⋯C distances (2.87 and 2.81 Å for Cr–C8 and Cr–C14, respectively) provide additional steric protection of the Cr atom, and the Cr–N(pyrrolyl) distance (2.0557(13) Å) is slightly longer than in **1-CrCl(thf)**.

Nevertheless, the most sterically encumbered pyrrolyl **3** in this series behaves differently. Deep-blue crystals were isolated from a 1 : 1 mixture of CrCl$_2$ and KPyr^{tBu_3} in THF (Scheme 4), but the ^{1}H NMR spectrum is distinctly different from those of **1-CrCl(thf)** and **2-CrCl(tmeda)**. Three resonances attributable to the three inequivalent tBu-groups are observed at δ 2.69, 6.68 and 12.17 ppm with similar line-width at half-height ($\nu_{1/2}$) of 573, 533 and 566 Hz, respectively. This suggests that in **3-CrCl** the pyrrolyl ligand is too sterically encumbered to allow κN-coordination; instead it shows η^5-coordination, as in the diazachromocene **3-Cr**. In addition, elemental analysis and EI mass spectrometry confirm the solvent-free, dimeric structure. Complex **3-CrCl** can also be prepared from **3-Cr** and CrCl$_2$.

Whereas X-ray investigations on **3-CrCl** confirmed the η^5-bonding mode, the N- and CH-positions within the pyrrolyl ring could not be unambiguously assigned during the refinement. To overcome this crystallographic difficulty, we decided to prepare the analogue half-sandwich complex with the 1,2,4-
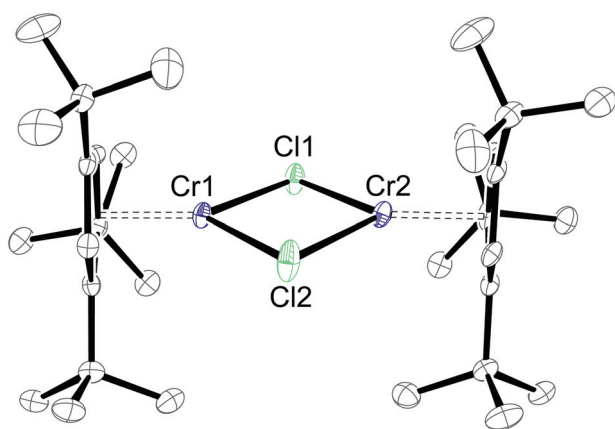
Scheme 4

Chart 2

Fig. 8 χ_T *vs.* T plot for **4-CrCl**. The red line represents a theoretical fit of the experimental data (see text for parameters).

Fig. 7 ORTEP diagram of **4-CrCl** with thermal displacement parameters drawn at 50% probability. The hydrogen atoms have been omitted for clarity. Selected bond lengths (Å) and angles (°): Cr1–Cl1 2.3542(6), Cr1–Cl2 2.3128(5), Cr2–Cl1 2.3093(5), Cr2–Cl2 2.3704(6), Cp(cent)–Cr 1.95, Cr1···Cr2 3.181; Cr1–Cl1–Cr2 86.019(18), Cl1–Cr2–Cl2 93.94(2), Cr1–Cl2–Cr2 85.567(19), Cl1–Cr1–Cl2 94.27(2).

$(Me_3C)_3C_5H_2$ (**4**) ligand, which we expected to be isostructural to **3-CrCl**. The reaction between $CrCl_2$ and $NaCp^{tBu_3}$ forms a green THF solution, and after work-up deep blue crystals are isolated from very concentrated pentane solutions at −24 °C (Scheme 4). Elemental analysis and EI MS data agree with the proposed structure for **4-CrCl**, but one particular observation for this complex is a solvent dependence of its solution colour and its ^1H NMR spectrum (see the Experimental section for details). In pentane and aromatic solvents green solutions are obtained, whereas it forms a blue solution in THF and CH_2Cl_2. Fig. 7 shows the molecular structure of **4-CrCl**, and the figure caption lists some selected bond distances and angles. Key features of the molecular structure include the long Cp(cent)–Cr distances of 1.95 Å and short Cr1···Cr2 distance of 3.181 Å, which is in the range of Cr–Cr bond distances (3.185–3.471 Å).[40] In principle, the Cr_2Cl_2-core can adopt two different structures, either a planar arrangement (**A**) or a butterfly geometry (**B**) (Chart 2). In the latter, the displacement of
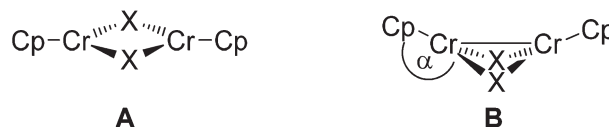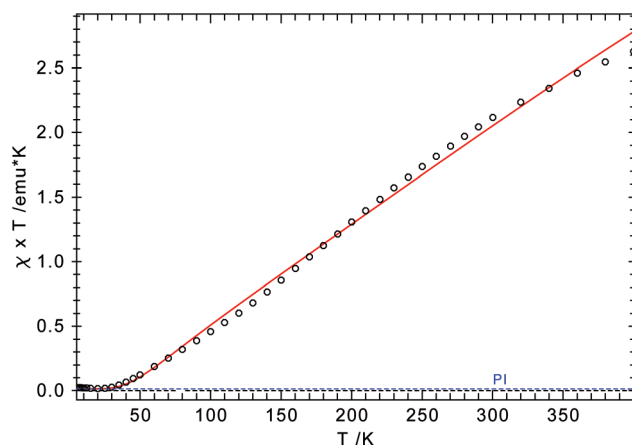
the two Cr atoms towards each other suggests a (weak) bonding interaction between the two Cr atoms.

Both arrangements have literature precedents. The butterfly structure is adopted in $[(\eta^5-C_5Me_5)Cr(\mu-X)]_2$ (X = Cl, Me),[41] $[(\eta^5-C_5Me_5)Cr(\mu-Et)(\mu-Ph)]_2$ (X = Cl, Me),[41] $[(\eta^5-C_5H_5)Cr(\mu-I)]_2$,[42] and $[(\eta^5-C_5H_5)Cr(\mu-OtBu)]_2$[43] and has direct consequences for the electronic structure of these dimers, which show strong antiferromagnetic coupling between the two Cr-atoms (S = 1).[41] In a more recent report, Layfield and Scheer describe a planar arrangement for $[(\eta^5-C_5H_5)Cr(\mu-X)]_2$ (X = $P(SiMe_3)_2$, As $(SiMe_3)_2$), in which two high spin (S = 2) Cr(II) centres couple antiferromagnetically.[40] To investigate the electronic structure in **4-CrCl**, magnetic susceptibility studies were undertaken between 5 and 400 K. The χ_T *vs.* T plot is shown in Fig. 8; and χ_T is close to zero at 5 K and then slowly increases to 2.6 emu K at 400 K. While this value is significantly less than the spin-only value of 6.0 emu K expected for two non-interacting high spin Cr(II) atoms (assuming g = 2), it is clearly higher than the expected value for two non-interacting S = 1 Cr(II) centers (2.0 emu K), suggesting antiferromagnetic coupling. The magnetic data can also be simulated by the spin-Hamiltonian $\hat{H} = -2J(\hat{S}_1 \cdot \hat{S}_2)$ with $S_1 = S_2 = 2$; $g_1 = g_2 = 2.41$; $J = -65.8$ cm^{-1}; TIP = 2.189×10^{-4} emu K and $\rho = 0.004$ (S = 2 impurity). These values are similar to those found for $[(\eta^5-C_5H_5)Cr(\mu-As-(SiMe_3)_2)]_2$.[40]

Catalytic screening in ethylene oligo-/polymerisation

With these Cr(II) complexes in hand, the activity of **2-CrCl-(tmeda)**, **3-CrCl** and **4-CrCl** in ethylene oligomerisation and polymerisation was investigated. This study should also provide insights into the influence of the pyrrolyl coordination

mode on the catalytic activity. The complexes were activated by addition of MAO or AlMe$_3$ in a 1 : 100 and 1 : 30 ratio, respectively. Furthermore 2 equiv. of dodecyltrimethylammonium chloride was added in the AlMe$_3$ reactions, since an external chloride source has some advantageous effects on the catalytic performance.[44] These mixtures were then heated to 50 °C under ethylene (30 bar). As shown in the previous study on **1-CrCl(thf)**,[18] these Cr(II) complexes are only poor catalysts in the selective ethylene polymerization and only trace amounts of oligomers are formed. However, there is a marked difference between the η^5-coordinate complexes **3-CrCl** and **4-CrCl** and the κN-bound complex **2-CrCl(tmeda)**. The former two complexes exhibit identical catalytic performance in olefin oligomerization (no selectivity and low activity of *ca.* 2 g h^{-1}) and no polyethylene formation regardless of the activator. In contrast **2-CrCl(tmeda)** forms polyethylene (*ca.* 12 g h^{-1}) on activation with MAO, but on activation with AlMe$_3$ no reaction occurs at 50 °C. However, when the temperature is raised to 75 °C a very slow reaction is initiated with very low ethylene consumption (<2 g h^{-1}) and most of the ethylene is converted to polyethylene. In conclusion, Cr(II) complexes with sterically encumbered pyrrolyl ligands are not suitable for the selective ethylene oligomerization, supporting the previous *in situ* EPR study, which established that only Cr(I) is relevant for the ethylene trimerization.[17]

Conclusions

Diazachromocenes with an $S = 1$ ground state are readily accessible from CrCl$_2$ and sterically encumbered pyrrolyl ligands. No indication of spin equilibrium was found based on solid state magnetic susceptibility studies for **1-Cr**. Reaction of the diazachromocenes with an additional equivalent of CrCl$_2$ forms mono(pyrrolyl) complexes, in which the Cr(II) atoms adopt a high spin ($S = 2$) ground state. In addition while κN-coordination is observed for **1-CrCl(thf)** and **2-CrCl(tmeda)**, this coordination mode is strongly disfavoured for the more sterically demanding Pyr^{tBu_3} ligand and therefore η^5-coordination is observed in **3-CrCl**. To distinguish these coordination modes ^{1}H NMR spectroscopy proved to be a very valuable tool. None of the mono(pyrrolyl)chromium complexes is a very active or selective ethylene oligomerization catalyst after activation with MAO or AlMe$_3$, strongly indicating that Cr(I)/Cr(III) are the important oxidation states in catalysis.

Further studies on the coordination chemistry of these pyrrolyl ligands are ongoing and will be reported in due course.

Experimental section

General

All synthetic and spectroscopic manipulations were carried out under an atmosphere of purified nitrogen, either in a Schlenk apparatus or in a glovebox. Solvents were dried and deoxygenated either by distillation under a nitrogen atmosphere from

sodium benzophenone ketyl (THF) or by an MBraun GmbH solvent purification system (all other solvents). NMR data were recorded on a Bruker DPX 200, a Bruker DRX 400, a Bruker Avance III 400 or a Bruker Avance II 300 spectrometer at ambient temperature unless stated otherwise. The residual solvent signal was used as a chemical shift reference ($\delta_H = 7.16$ for benzene, 7.26 for chloroform, 3.58 for α-H of THF) for the ^{1}H spectra and the solvent signal ($\delta_C = 128.06$ ppm for benzene, 77.17 for chloroform, 67.21 for α-C of THF) for the ^{13}C spectra. Elemental analyses were performed by combustion and gas chromatographic analysis with an Elementar vario-MICRO instrument. Magnetic measurements were conducted in a 7 T Quantum Design MPMS magnetometer utilizing a superconducting quantum interference device (SQUID). Between 10 and 25 mg of the sample were sealed in evacuated quartz tubes held in place with ~5 mg of quartz wool. This method provided a very small and reliable container correction, typically of about -2×10^{-5} emu mol^{-1}. The data were also corrected for the overall diamagnetism of the molecule using Pascal constants.[45] For a more detailed description see ref. 46. The program package JulX was used for spin-Hamiltonian simulations and fitting of the data by a full-matrix diagonalization approach.[47] NaPyr^{tBu_2} (**1-Na**),[48] KPyr^{tBu_2Me_2} (**2-K**),[22] KPyr^{tBu_3} (**3-K**)[22] and NaCp^{tBu_3} (**4-Na**)[49] were prepared according to the literature procedures.

Synthesis of 2,2′,5,5′-tetra-*tert*-butyl-diazachromocene (1-Cr). A solution of NaPyr^{tBu_2} (0.329 g, 1.62 mmol) in THF (10 mL) was added to a suspension of CrCl$_2$ (0.100 g, 0.81 mmol) in THF (10 mL). The mixture turned red-brown and was stirred overnight at ambient temperature and filtered over Celite. The solvent was removed under dynamic vacuum and the residue was extracted with pentane. The extracts were concentrated and cooled to −24 °C to give the product as dark-red needles. Yield: 0.208 g (0.51 mmol, 63%). M.p. 105–114 °C. ^{1}H NMR (300 MHz, C$_6$D$_6$, 298 K): δ 1.99 (br. s, $\nu_{1/2}$ = 121 Hz, C(C*H*$_3$)$_3$) ppm. Resonances corresponding to the C*H* protons were not observed. Anal. Calcd for C$_{24}$H$_{40}$N$_2$Cr (408.26): C, 70.55; H, 9.87; N, 6.86. Found: C, 69.69; H, 9.67; N, 6.56. μ_{eff} = 3.02μ_B (300 K, solid).

Synthesis of 2,2′,5,5′-tetra-*tert*-butyl-3,3′,4,4′-tetramethyldi-azachromocene (2-Cr). A solution of KPyr^{tBu_2Me_2} (0.500 g, 2.04 mmol) in THF (20 mL) was added dropwise to a suspension of CrCl$_2$ (0.125 g, 1.02 mmol) in THF (15 mL). The mixture turned from green to red-brown and was refluxed for 5 h and then stirred overnight at room temperature. The residue was extracted with hexane, filtered and the solvent was removed under a dynamic vacuum to give a red solid. Yield: 0.320 g (0.69 mmol, 68%). Crystals suitable for X-ray diffraction analysis were grown from a concentrated hexane solution at −24 °C overnight. M.p. 236–245 °C. ^{1}H NMR (300 MHz, C$_6$D$_6$, 298 K): δ 5.36 (br. s, $\nu_{1/2}$ = 334 Hz, C*H*$_3$), −0.47 (br. s, $\nu_{1/2}$ = 264 Hz, C(C*H*$_3$)$_3$ ppm. Anal. Calcd for C$_{28}$H$_{48}$N$_2$Cr (464.32): C, 72.37; H, 10.41; N, 6.03. Found: C, 71.62; H, 10.08; N, 5.83.

Synthesis of 2,2′,3,3′,5,5′-hexa-*tert*-butyl-diazachromocene (3-Cr). A solution of KPyr^{tBu_3} (0.500 g, 1.83 mmol) in THF (10 mL) was added to a suspension of CrCl$_2$ (0.112 g,

0.91 mmol) in THF (10 mL). The mixture turned from blue *via* green to red-brown and was stirred at ambient temperature overnight. The solvent was removed under dynamic vacuum. The residue was extracted with hexamethyldisiloxane. Concentration to a minimum amount of solvent and crystallization at -24 °C gave red-brown crystals. Yield: 0.202 g (0.37 mmol, 40%). M.p. 252 °C (dec.). ^{1}H NMR (200 MHz, C_6D_6, 300 K): δ 3.63 (br. s, $\nu_{1/2} = 408$ Hz, $C(CH_3)_3$, peak overlap), 1.55 (br. s, $\nu_{1/2} = 163$ Hz, $C(CH_3)_3$, peak overlap), 0.38 (br. s, $\nu_{1/2} = 113$ Hz, $C(CH_3)_3$, peak overlap) ppm. Anal. Calcd for $C_{32}H_{56}N_2Cr$ (520.38): C, 73.80; H, 10.84; N, 5.38. Found: C, 73.55; H, 10.84; N, 5.41. The E.I. mass spectrum (70 eV) showed a molecular ion at $m/z = 520$ amu with the following isotopic cluster distribution for: $C_{32}H_{56}N_2Cr$ (calcd %, observd %): 520 (100, 100), 521(47, 46), 522 (13, 13), 518 (5, 5), 523 (2, 2).

Synthesis of [{(κN-2,5-(Me₃C)₂C₄H₂N)Cr(thf)}₂(μ-Cl)₂] (1-CrCl(thf)). A solution of NaPyr^{tBu_2} (1.000 g, 4.94 mmol) in THF (20 mL) was added to a suspension of $CrCl_2$ (0.608 g, 4.94 mmol) in THF (25 mL). The mixture turned blue-green and was stirred overnight and filtered over Celite. The solvent was concentrated to *ca.* 15 mL and the product was precipitated by the pentane addition. The product was dried *in vacuo* to give a light blue solid. Yield: 1.121 g (1.66 mmol, 67%). Crystals suitable for X-ray diffraction were obtained as blue cubes by slow vapour diffusion of pentane into a concentrated THF solution of **1-CrCl(thf)**. M.p. 138 °C (dec.). ^{1}H NMR (400 MHz, THF-d_8, 299 K): $\delta = 55.4$ (br. s, $\nu_{1/2} = 2580$ Hz, 9H, $C(CH_3)_3$), -28.4 (br. s, $\nu_{1/2} = 400$ Hz, 1H, CH) ppm. Anal. Calcd for $C_{32}H_{56}N_2O_2Cl_2Cr$ (674.52): C, 56.88; H, 8.35. Found: C, 56.37; H, 8.39. $\mu_{eff} = 7.00\mu_B$ (300 K, solid).

Synthesis of [(κN-2,5-(Me₃C)₂-3,4-Me₂-C₄H₂N)Cr(Cl)(tmeda)] (2-CrCl(tmeda)). To a suspension of $CrCl_2$ (0.150 g, 1.22 mmol) in THF (20 mL), tmeda (*ca.* 2 mL) was added and a solution of KPyr^{tBu_2Me_2} (0.300 g, 1.22 mmol) in THF (20 mL) was added dropwise. The mixture turned from green to steel-blue and was stirred overnight and filtered. The solvent was concentrated until a blue precipitate formed and the suspension was kept at -24 °C for 2 h. The green supernatant was decanted and the blue solid was washed with pentane and recrystallized from THF at -24 °C. Yield: 0.150 g (0.37 mmol, 30%). M.p. 161–178 °C (dec.). ^{1}H NMR (300 MHz, THF-d_8, 296 K): δ 37.8 (br. s, $\nu_{1/2} = 260$ Hz, $C(CH_3)_3$), 2.3 (br. s, $\nu_{1/2} = 50$ Hz, peak overlap), 2.2 (br. s, $\nu_{1/2} = 66$ Hz, peak overlap) ppm. Anal. Calcd for $C_{20}H_{40}N_3ClCr$ (409.23): C, 58.59; H, 9.83; N, 10.25. Found: C, 58.15; H, 9.93; N, 10.07.

Synthesis of [(η⁵-2,3,5-(Me₃C)₃C₄HN)Cr(μ-Cl)₂] (3-CrCl). A solution of KPyr^{tBu_3} (0.500 g, 1.83 mmol) in THF (20 mL) was added to a suspension of $CrCl_2$ (0.223 g, 1.83 mmol) in THF (20 mL). The mixture changed in colour from green to blue and was stirred overnight. The solvent was evaporated and the residue was extracted with hexane. Concentration to a minimum amount of solvent and crystallization at -24 °C gave deep-blue crystals. Yield: 0.238 g (0.37 mmol, 40%). M.p. 147–150 °C (dec.). ^{1}H NMR (400 MHz, C_6D_6, 298 K): δ 2.69 (br. s, $\nu_{1/2} = 573$ Hz, $C(CH_3)_3$), 6.68 (br. s, $\nu_{1/2} = 533$ Hz, $C(CH_3)_3$), 12.17 (br. s, $\nu_{1/2} = 566$ Hz, $C(CH_3)_3$) ppm. The CH resonance

was not observed. Anal. Calcd for $C_{32}H_{56}N_2Cl_2Cr$ (642.26): C, 59.71; H, 8.77; N, 4.35. Found: C, 59.63; H, 8.71; N, 4.26. The E.I. mass spectrum (70 eV) showed a molecular ion at $m/z = 642$ amu with the following isotopic cluster distribution for: (calcd %, observd %): 642 (100, 100), 644 (82, 82), 643 (58, 60), 645 (40, 40), 646 (22, 23), 640 (10, 11), 647 (9, 9), 641 (4, 5), 648 (2, 3).

Synthesis of [(η⁵-1,2,4-(Me₃C)₃C₅H₂)Cr(μ-Cl)₂] (4-CrCl). In a Schlenk flask, NaCp^{tBu_3} (1.024 g, 4.00 mmol) and $CrCl_2$ (0.492 g, 4.00 mmol) were suspended in THF (*ca.* 30 mL) and the reaction mixture was stirred at ambient temperature for 2 d. During this time the $CrCl_2$ slowly dissolved and a blue solution was formed. The solvent was evaporated and the residue was extracted with pentane (*ca.* 20 mL). The green pentane extracts were filtered and concentrated to *ca.* 5 mL and cooled to -24 °C to give deep blue crystals. Yield: 0.55 g (0.86 mmol, 43%). M.p. 151–156 °C. ^{1}H NMR (200 MHz, C_6D_6, 296 K, green solution): δ 10.61 (br. s, peak overlap), 9.10 (br. s, peak overlap) ppm. ^{1}H NMR (200 MHz, CD_2Cl_2, 296 K, blue solution) 3.17 (shoulder, peak overlap), 2.07 (br. s, peak overlap) ppm. Anal. Calcd for $C_{34}H_{58}Cl_2Cr_2$ (640.27): C, 63.64; H, 9.11. Found: C, 63.22; H, 9.21. The E.I. mass spectrum (70 eV) showed a molecular ion at $m/z = 640$ amu with the following isotopic cluster distribution for: (calcd %, observd %): 640 (100, 100), 642 (82, 80), 641 (59, 59), 643 (41, 41), 644 (24, 25), 638 (10, 14), 645 (9, 10), 639 (5, 8), 646 (3, 3).

X-ray diffraction studies

Data were recorded at 100 K on Oxford Diffraction diffractometers using monochromated Mo Kα or mirror-focussed Cu Kα radiation (Table 1). Absorption corrections were performed on the basis of multi-scans. The structures were refined anisotropically using the SHELXL-97 program.[50] Hydrogen atoms were included using rigid idealised methyl groups or a riding model. *Special features and exceptions*: **1-Cr** was refined as a racemic twin (Flack parameter 0.17(2)). **2-Cr** was measured at 130 K because the crystals shatter at 100 K.

Acknowledgements

Notes and references

1 K. H. Pannell, B. L. Kalsotra and C. Párkányi, *J. Heterocycl. Chem.*, 1978, **15**, 1057–1081.

2 L. Kollar and G. Keglevich, *Chem. Rev.*, 2010, **110**, 4257–4302.

3 A. J. Ashe and S. A. Al-Ahmad, *Adv. Organomet. Chem.*, 1996, **39**, 325–353.

4 (a) F. Mathey, *Nouv. J. Chim.*, 1987, **11**, 285; (b) D. Carmichael and F. Mathey, *Top. Curr. Chem.*, 2002, **220**, 27–51, and references cited therein; (c) P. Le Floch, *Coord. Chem. Rev.*, 2006, **250**, 627–681.

5 K. B. Dillon, F. Mathey and J. F. Nixon, *Phosphorus. The carbon copy; from organophosphorus to phospha-organic chemistry*, John Wiley, Chichester, 1998.

6 N. Kuhn, *Bull. Soc. Chim. Belg.*, 1990, **99**, 707–715.

7 C. Janiak and N. Kuhn, *Adv. Nitrogen Heterocycl.*, 1996, **2**, 179–210.

8 D. L. Kershner and F. Basolo, *J. Am. Chem. Soc.*, 1987, **109**, 7396–7402.

9 R. V. Bynum, H. M. Zhang, W. E. Hunter and J. L. Atwood, *Can. J. Chem.*, 1986, **64**, 1254–1257.

10 F. Nief, *Eur. J. Inorg. Chem.*, 2001, 891–904.

11 D. Tille, *Z. Naturforsch., B: Anorg. Chem. Org. Chem. Biochem. Biophys. Biol.*, 1966, **21**, 1239.

12 D. Tille, *Z. Anorg. Allg. Chem.*, 1971, **384**, 136–146.

13 J. J. H. Edema, S. Gambarotta, A. Meetsma, B. F. Van, A. L. Spek and W. J. J. Smeets, *Inorg. Chem.*, 1990, **29**, 2147–2153.

14 W. M. Woodard, W. M. Ewert, H. D. Hensley, M. E. Lashier, B. E. Kreischer, G. D. Cowan, J. W. Freeman, R. V. Franklin, R. D. Knudsen, R. L. Anderson and L. R. Kallenbach, *Process and catalyst system for the trimerization of olefins*, WO9919280A1, 1999.

15 J. T. Dixon, M. J. Green, F. M. Hess and D. H. Morgan, *J. Organomet. Chem.*, 2004, **689**, 3641–3668.

16 R. W. J. Van, C. Grove, J. P. Steynberg, K. B. Stark, J. J. Huyser and P. J. Steynberg, *Organometallics*, 2004, **23**, 1207–1222.

17 I. Y. Skobelev, V. N. Panchenko, O. Y. Lyakin, K. P. Bryliakov, V. A. Zakharov and E. P. Talsi, *Organometallics*, 2010, **29**, 2943–2950.

18 S. Licciulli, K. Albahily, V. Fomitcheva, I. Korobkov, S. Gambarotta and R. Duchateau, *Angew. Chem., Int. Ed.*, 2011, **50**, 2346–2349.

19 N. Kuhn, G. Henkel, J. Kreutzberg, S. Stubenrauch and C. Janiak, *J. Organomet. Chem.*, 1993, **456**, 97–106.

20 C. Janiak, N. Kuhn and R. Gleiter, *J. Organomet. Chem.*, 1994, **475**, 223–227.

21 M. Kreye, J. W. Runyon, M. Freytag, P. G. Jones and M. D. Walter, *Dalton Trans.*, 2013, **42**, 16846–16856.

22 M. Kreye, A. Glöckner, C. G. Daniliuc, M. Freytag, P. G. Jones, M. Tamm and M. D. Walter, *Dalton Trans.*, 2013, **42**, 2192–2200.

23 M. Kreye, D. Baabe, P. Schweyen, M. Freytag, C. G. Daniliuc, P. G. Jones and M. D. Walter, *Organometallics*, 2013, **32**, 5887–5898.

24 P. Crewdson, S. Gambarotta, M.-C. Djoman, I. Korobkov and R. Duchateau, *Organometallics*, 2005, **24**, 5214–5216.

25 I. Korobkov and S. Gambarotta, *Organometallics*, 2009, **28**, 5560–5567.

26 M. Schultz, *Acta Crystallogr., Sect. E: Struct. Rep. Online*, 2007, **63**, m3085.

27 L. Pauling, *The Nature of the Chemical Bond*, Cornell University Press, Ithaka, New York, 1960.

28 A. Hildebrandt, D. Schaarschmidt, R. Claus and H. Lang, *Inorg. Chem.*, 2011, **31**, 10623–10632.

29 A. Hildebrandt and H. Lang, *Dalton Trans.*, 2011, **40**, 11831–11837.

30 D. Miesel, A. Hildebrandt, M. Korb, P. J. Low and H. Lang, *Organometallics*, 2013, **32**, 2993–3002.

31 R. Bartsch, P. B. Hitchcock and J. F. Nixon, *J. Organomet. Chem.*, 1988, **356**, C1–C4.

32 T. J. Brunker, J. C. Green and D. O'Hare, *Inorg. Chem.*, 2002, **41**, 1701–1703.

33 T. J. Brunker, J. C. Green and D. O'Hare, *Inorg. Chem.*, 2003, **42**, 4366–4381.

34 J. S. Overby, N. J. Schoell and T. P. Hanusa, *J. Organomet. Chem.*, 1998, **560**, 15–19.

35 (a) H. Sitzmann, M. Schär, E. Dormann and M. Kelemen, *Z. Anorg. Allg. Chem.*, 1997, **623**, 1850–1852; (b) H. Sitzmann, *Coord. Chem. Rev.*, 2001, **214**, 287–327.

36 R. D. Fischer, in *NMR of Paramagnetic Molecules*, ed. G. N. La Mar, W. D. Horrocks and R. H. Holm, Academic Press, New York, 1973, pp. 521–553.

37 D. C. Bradley, M. B. Hursthouse, C. W. Newing and A. J. Welch, *J. Chem. Soc., Chem. Commun.*, 1972, 567–568.

38 J. N. Boynton, W. A. Merrill, W. M. Reiff, J. C. Fettinger and P. P. Power, *Inorg. Chem.*, 2012, **51**, 3212–3219.

39 C. W. Bird and G. W. H. Cheeseman, in *Comprehensive Heterocycles*, ed. A. R. Katritzky and C. W. Rees, Pergamon Press, Oxford, 1984, pp. 1–10.

40 S. Scheuermayer, F. Tuna, E. M. Pineda, M. Bodensteiner, M. Scheer and R. A. Layfield, *Inorg. Chem.*, 2013, **52**, 3878–3883.

41 R. A. Heintz, R. L. Ostrander, A. L. Rheingold and K. H. Theopold, *J. Am. Chem. Soc.*, 1994, **116**, 11387–11396.

42 M. E. Burin, M. V. Smirnova, G. K. Fukin, E. V. Baranov and M. N. Bochkarev, *Eur. J. Inorg. Chem.*, 2006, **2006**, 351–356.

43 M. H. Chisholm, F. A. Cotton, M. W. Extine and D. C. Rideout, *Inorg. Chem.*, 1979, **18**, 120–125.

44 B. H. Müller, N. Peulecke, S. Peitz, B. R. Aluri, U. Rosenthal, M. H. Al-Hazmi, F. M. Mosa, A. Wöhl and W. Müller, *Chem. – Eur. J.*, 2011, **17**, 6935–6938.

45 C. J. O'Connor, in *Progress in Inorganic Chemistry*, ed. S. J. Lippard, J. Wiley & Sons, New York, 1982, vol. 29, pp. 203–285.

46 M. D. Walter, M. Schultz and R. A. Andersen, *New J. Chem.*, 2006, **30**, 238–246.

47 E. Bill, http://www.cec.mpg.de/forschung/molekulare-theorie-und-spektroskopie-molecular-theory-and-spectroscopy/moessbauer-mcd.html.

48 H. Schumann, J. Winterfeld, H. Hemling and N. Kuhn, *Chem. Ber.*, 1993, **126**, 2657–2659.

49 M. D. Walter, C. D. Sofield, C. H. Booth and R. A. Andersen, *Organometallics*, 2009, **28**, 2005–2019.

50 (a) G. M. Sheldrick, *SHELXL-97, Program for the Refinement of Crystal Structure from Diffraction Data*, University of Göttingen, Göttingen, Germany, 1997; (b) G. M. Sheldrick, *Acta Crystallogr., Sect. A: Fundam. Crystallogr.*, 2008, **64**, 112–122.